

# Viscous instabilities in flowing foams: A Cellular Potts Model approach.

Soma Sanyal and James A. Glazier<sup>y</sup>

BioComplexity Institute, Department of Physics,  
Indiana University, Bloomington, IN 47405

## Abstract

The Cellular Potts Model (CPM) successfully simulates foam drainage and stress and strain in sheared foams. Here we use the CPM to investigate instabilities due to the flow of a single large bubble in a dry, monodisperse two-dimensional flowing foam. As in experiments, above a threshold velocity, the large bubble moves faster than the mean flow. Our simulations reproduce analytical and experimental prediction for the velocity threshold and the relative velocity of the large bubble moving in a Hele-Shaw cell, demonstrating the utility of the CPM in foam rheology studies.

PACS numbers: PACS numbers: 83.80.Iz, 83.50.-v, 05.50.+q, 47.50.+d

---

<sup>x</sup> e-mail: ssanyal@indiana.edu

<sup>y</sup> e-mail: glazier@indiana.edu

Foam's unusual rheology gives them applications in diverse fields, from efficient extinguishers to oil extraction in the petroleum industry [1, 2]. Foams are non-Newtonian, so the study of their flow helps explain the complex behaviour of structured fluids, which is difficult to investigate analytically. Though we know that foams behave like solids under small stress and flow like fluids under large stress, we still do not understand the relationship between the macroscopic and microscopic properties of foams. Thus we must design experiments and simulations which provide insight into foam-flow behaviour [3, 4]. In this paper, we restrict ourselves to two dimensional foams. We also consider dry foams, i.e. foams where the fluid fraction is negligible. We show that the CPM can successfully model foam flow in a Hele Shaw (H-S) cell, i.e. a single bubble layer flow between two closely spaced long and narrow parallel plates. The foam flows between the plates parallel to the length, producing a quasi-two-dimensional flow. H-S flow is important in industrial processes such as injection molding [16] and display device design [17].

The sizes and shapes of the bubbles forming a foam may change due to gas diffusion between neighbouring bubbles, bubble coalescence, shear and drainage of liquid between bubble walls [5]. In this paper we consider only shear induced T1 processes, where two bubbles come together to share a side, pushing apart two previously adjacent bubbles [6]. If a large number of T1s occur together, with each T1 triggering the next, they form an avalanche. This kind of collective bubble rearrangements which occur during foam flow have inspired many models. The most important are the constitutive, vertex, center, bubble and Cellular Potts (CPM) models ([7]–[14]). For example, Okuzano and Kawasaki used a vertex model to study the effect of low shear rates on foams [1] and found avalanche-like rearrangements. Durian's bubble model [12] gave similar predictions but Weaire's center model [13] suggested that avalanche-like rearrangements are only possible for wet foams. Jiang et al. tried to reconcile the different model predictions and experiments using the CPM (extended to include shear) [15]; which also successfully models foam coarsening and drainage [14]. They demonstrated hysteresis and avalanche-like rearrangements in a two-dimensional non-coarsening foam and found that the dynamics of topological rearrangements depended sensitively on any deviations from the ideal, regular, hexagonal structure of the bubbles in the foam. However, because the CPM derives from an equilibrium model, doubt arises about its suitability to describe dynamic phenomena. Here we show that the CPM correctly reproduces the rather subtle experimental behaviour of the flow of a large bubble

in a background of small bubbles.

For H-S flow of a monodisperse foam (i.e. a foam made of bubbles of equal size), under an uniform pressure gradient, the flow is a simple plug flow. However for a polydisperse foam (i.e. foam made of bubbles of different sizes), the flow becomes unstable above a critical velocity. The size distribution of the bubbles then controls the velocity field, with the larger bubbles moving faster than the smaller ones, as experiments by Lordereau [18] have shown. Recently Cantat and Delannay [19] studied the phenomenon in more detail, both experimentally and numerically. Their experiments used a dry soap froth contained between two horizontal plates, where newly produced bubbles maintained a steady pressure gradient across the length of the H-S cell. Their simulations used a vertex model with periodic boundary conditions along the direction of flow. They also made analytical predictions which agree with their numerical and experimental results for the critical velocity for a single large bubble to move faster than the bulk flow in an otherwise monodisperse foam.

According to Cantat and Delannay [19], below the critical velocity, all the bubbles in the foam move with a velocity  $v_0 u_x$  where  $u_x$  is a unit vector in the direction of flow. The viscous force per unit surface, averaged on the scale of a bubble, is:

$$F_{visc} = -\frac{v_0}{d} u_x; \quad (1)$$

where  $\eta$  is the effective viscosity and  $d$  is the diameter of the small bubbles. The large bubble induces a pressure deficit  $f = n \eta u_x$  where  $n$  is the number of lamellae that would be present across the large bubble in the  $x$  direction if filled with small bubbles. Assuming the friction deficit concentrates at  $r = \frac{d}{2}$ , the force equation becomes,

$$F_{visc} = -r \frac{v_0 x}{d} + (r - r_0) \frac{v_0 D^2}{d} u_x; \quad (2)$$

where  $D$  is the diameter of the large bubble. As the large bubble moves it distorts the arrangement of the small bubbles and the stress due to surface tension of the individual bubbles change. Combining the forces due to surface tension and viscosity, Cantat and Delannay [19] obtained the equations of motion:

$$r \left( \frac{v_0 x}{d} + P \right) + r^2 x = (r - r_0) \frac{v_0 D^2}{d} u_x; \quad (3)$$

$$r \ddot{x} = 0; \quad (4)$$

where  $P$  is the pressure field given by,

$$P = -\frac{v_0 x}{d} + \frac{v_0 D^2}{2d} \frac{x - x_0}{(r - r_0)^2}; \quad (5)$$

for the small bubbles. The last term on the R.H.S of equation (5) gives the pressure discontinuity for the larger bubble at  $r = \frac{D}{2u_x}$ , which must counterbalance the stress. The force balance gives the critical velocity:

$$v_c = \frac{\gamma}{D}; \quad (6)$$

where  $\gamma$  is the surface tension. The critical velocity is directly proportional to the surface tension and inversely proportional to the diameter of the large bubble and the viscosity.

In this work we use the CPM to reproduce large-bubble migration. Our results agree with the results obtained in ref. [19]. The CPM simulations are simple. The dissipation results from energy minimization. The limitation of the CPM is our inability to determine the viscosity analytically in terms of model parameters. We can still obtain an effective viscosity and other viscoelastic information from our simulations, (e.g. by determining the critical velocity above which a large bubble moves faster than the surrounding smaller bubbles). Our simulations validate the use of the CPM for studying foam rheology.

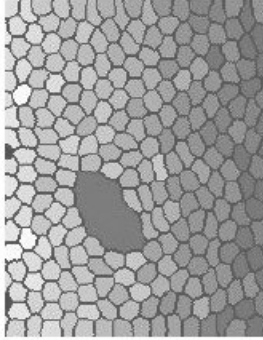
Since Jiang et al. [15] have used the CPM to study foam rheology we need not dwell on the details of the model. The CPM is lattice-based, with each lattice point having an integer spin. Like spins form bubbles while boundaries between unlike spins correspond to soap films. The CPM Hamiltonian contains a surface energy term corresponding to the surface tension and, since we focus on the motion of bubbles of fixed sizes, a term constraining bubble areas to prevent foam coarsening. The Hamiltonian thus has two terms:

$$H = \sum_{i,j}^X J(1 - \delta_{i,j}) + \sum_n^X (a_n - A_n)^2; \quad (7)$$

where  $J$  is the coupling strength between neighbouring spins  $i, j$  at lattice sites  $i$  and  $j$  and  $\delta$  is the strength of the area constraint.  $A_n$  is the area of a bubble with no forces (including surface tension) acting on it, which we call the target area while  $a_n$  is the current area of the same bubble as it flows. The first term gives the total surface energy and the second term the pressure energy. The area constraint is inversely proportional to the gas compressibility, so the model obeys the ideal gas law. The difference between the areas  $(a_n - A_n)$  gives the pressure in the bubble. The CPM spins evolve according to a Model

Metropolis algorithm [15]. Each time step corresponds to a complete Monte Carlo Sweep (MCS) of the lattice.

Fig. 1 shows a snapshot of the simulation with the large bubble moving through the smaller bubbles. The shades denote the pressure inside each bubble, darker shades denoting lower pressures. The bubbles move from left to right. We use open boundary conditions at the short ends of the lattice to simulate the flow. We nucleate bubbles at one short end and allow them to disappear at the other short end. All the bubbles, except the large bubble are nucleated at a fraction of their target area. As they expand to their target area they generate a pressure on the foam in the channel. The flow is due to the pressure gradient the nucleated bubbles generate. The initial size of the nucleated bubbles and the nucleation rate determine this gradient. Since the size of the short end of the lattice is fixed and bubbles are generated all along it, the number of bubbles nucleated varies with the initial size of the bubble. We change the pressure gradient by generating bubbles of different initial sizes at a fixed interval. At the other end of the channel, we relax the area constraint so that the bubbles collapse and disappear. This method of bubble creation and disappearance corresponds closely to the experiments which generate bubbles continuously at one end of the channel and allows them to exit at the opposite end. Thus the simulation and the experiment both have constant bubble flux boundary condition at one end and absorbing boundary condition at the other.



Direction of flow -->

FIG. 1:

The figure shows part of a CPM simulation of a quasi-stationary flowing foam with a large bubble. The different shades denote bubble pressures with darker shades denoting lower pressures.

We track the centre of mass of each bubble at each time step. We use a lattice of 1000 X 200 for most of our simulations. The smaller bubble contains 625 lattice sites. We vary the large bubble size. If the large bubble radius is more than four times the radius the small bubble, we use a larger lattice size to avoid boundary effects. The simulations use  $J = 5$  and  $\gamma = 3$  and run at zero temperature. The velocity of the foam depends upon  $J$  and  $\gamma$  which relate to the viscosity and surface tension of the foam, and on the rate at which we add new bubbles at the end of the channel. We track the large bubble and one of the smaller bubbles. The smaller bubbles all have approximately the same velocity at any given time and we choose any bubble to track randomly. However the average velocity of the foam is less than the velocity of any individual bubble at any given time. This difference in average foam velocity and individual bubble velocity remains constant for a particular velocity.

As in refs. [11] and [15] we define the total stored surface energy as,

$$\sigma = \frac{1}{2} \sum_{i,j} \gamma_{i,j} \quad (8)$$

The average stress tensor as ref. [11] points out relates directly to  $\sigma = \text{Tr}(\sigma)$ . We scale out the differences due to initial conditions by using  $\frac{\sigma(t)}{\sigma(0)}$ , where  $\sigma(0)$  is the value of  $\sigma$  at the start of the simulation. The applied strain rate, is very high initially, then falls sharply to a low value which remains constant so the applied strain is proportional to time. The energy vs time curve becomes equivalent to the energy vs applied strain curve.

The foam begins to flow when we apply a pressure gradient across it, if we maintain the constant pressure difference for a longer period of time, the foam flow gradually settles down to a quasi-stationary state. We call it quasi-stationary when the change in the energy of the system becomes less than 2 % of the average energy over 1000 MCS. When we refer to the velocity of a bubble we mean the velocity in its quasistationary state. The bubble velocity at this stage changes by about 10 % of the average velocity over 1000 MCS. Fig 2 (a) plots as a function of time and Fig 2 (b) plots the velocity of large and small bubbles as a function of time. For any velocity and radius, simulations are run for different seeds and different initial large bubble positions on the short end. We create only one large bubble having a diameter  $D$  in the first time step at any position along the short end through which the rest of the bubbles enter. We nucleate small bubbles after every 50 time steps and track the velocity of the large bubble and a smaller bubble adjacent to it. We vary the velocity by varying the initial size of the nucleated bubbles from 481 pixels to 4 pixels. Velocity of the

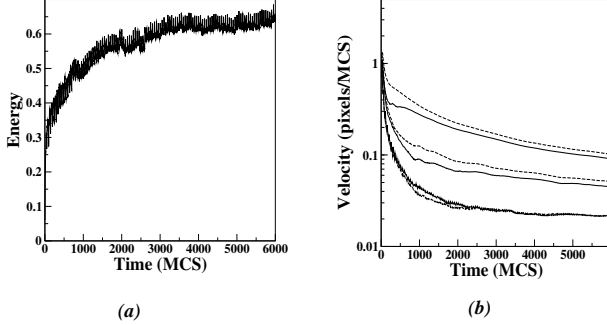


FIG .2:

(a) The evolution of the energy of a flowing foam containing a large bubble with new bubbles nucleating every 50 MCS.

(b) Bubble velocity for in a simulated two-dimensional flowing foam : large bubble-dashed lines, small bubbles-solid lines. The three pairs of curves are for different nucleation sizes of small bubbles. The lowest curve corresponds to an initial nucleation size of 481 pixels and the other two curves to nucleation sizes of 156 and 25 pixels respectively.

bubbles are higher for smaller nucleation sizes.

As the velocity increases, we gradually reach the critical velocity beyond which the bubble velocities depend on their sizes. From our simulations we find that the critical velocity is 0.026 pixels/mcs, when the radius of the large bubble is twice that of the small bubble. We then plot the difference in velocity between the large and small bubbles ( $v_L - v_s$ ) vs the velocity of the small bubbles  $v_s$  for different large-bubble sizes  $D$ , scaling the velocity difference by  $r = D/d$ , where the diameter of the small bubble  $d$  is kept constant. Fig 3 shows that our results agree with those of Cantat and Delanney [19]. We find a critical velocity ( $v_c$ ), beyond which the velocity of large bubbles depends on their size  $D$ . We also check that  $v_c$  does not depend on  $d$  by running simulations with the small bubble size 400 pixels. We examine  $r = 2; 3; 3.5; 4$ . Large bubbles tend to wobble and break into smaller bubbles. We consider only simulations in which the large bubble traverses the H-S cell without breaking, limiting our statistics for higher  $r$  ratios. We fit our data using least squares to the theoretical prediction of Cantat and Delanney [19];

$$\frac{(v_L - v_s)}{v_s (D=d)} = \frac{A}{v_s} - \frac{1}{B \ln(1 - \frac{A}{v_s})}; \quad (9)$$

where  $(v_L - v_s)$  is the difference between the large and small bubbles velocities and  $A$  and  $B$

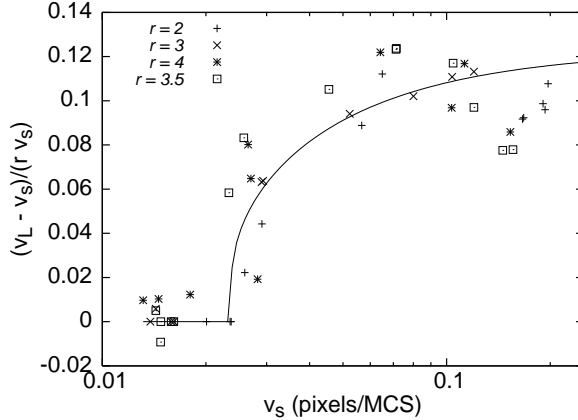


FIG . 3:

Difference between large bubble velocity  $v_L$  and small bubble velocity  $v_s$  for different radii of the large bubble, rescaled by  $rv_s$  on a semi log axes. The different symbols on the graph correspond to different  $r$ .

are the fitting parameters.  $A$  corresponds to the critical velocity of 0.024 pixels/MCS. This matches very well with the  $v_c$  we had obtained for  $r = 2$  separately from our simulations.  $B$  is a dimensionless parameter which scales the velocity,  $B = 8.10$ . Though the points appear to scatter, the asymptotic standard error for both parameters is less than 5%.

The theoretical critical velocity is [19]:

$$v_c = \frac{h}{D}; \quad (10)$$

where  $h$  is the thickness of the H-S cell. Assuming  $h$  to be the small bubble size, we obtain  $v_c$  from values of  $h$  and  $D$  obtained from our simulations. We obtain  $h$  from the effective pressure across the channel and the corresponding velocity and  $D$  from the size and pressure of the small bubbles. We get  $v_c = 0.014$  pixels/MCS. The discrepancy of our theoretical and simulation value arises from the assumption of  $h$ .  $h$  in our simulations is assumed to be infinitely small while in the theoretical calculation we take it to be the small bubble size.

In summary, we have shown that we can use the CPM to study the flow of a large bubble embedded in a monodisperse foam. We see that for small velocities, all the bubbles in the foam flow with the same velocity. Above a critical velocity, the velocities of the bubbles vary with their sizes. We obtain the critical velocity from our detailed simulations when the large bubble is twice the size of the small bubble. This matches very well with the value we get by graphically fitting the analytical equation obtained by Cantat and Dellenay [9], using the critical velocity as a fitting parameter for bubbles of various sizes. We also obtained the

critical velocity theoretically from the effective viscosity and surface tension of the foam in the simulation. There was a discrepancy in the two values as (our simulations being two dimensional), we had to assume a value for the thickness of the H-S cell for our theoretical calculation.

We have shown that the critical velocity depends on the large bubble size, however we have not checked the dependency of the critical velocity on the surface tension and viscosity. We plan to do this in a future work. We have also checked that for a polydisperse foam above a certain velocity different bubbles travel with different velocities depending on their sizes; the largest bubble traveling the fastest. The present definition of the critical velocity indicates that bubbles of different sizes will have different critical velocities. We find it difficult to verify this for the polydisperse foam as the scatter in the velocity difference is very large and the critical velocity cannot be identified definitely. Our study indicates that the CPM can reveal different aspects of foam rheology. For example, we are presently using the CPM to study this Saffman-Taylor instability in foams. Since these instabilities are important in industry, a better understanding of these are very useful.

Acknowledgments: We acknowledge the use of AVADD, the distributed computing facility at Indiana University Bloomington to run our simulations. We thank Debasis Das, Ariel Balter, Lenhilton Coutinho, Roeland Merks and Julio Espinoza Ortiz for discussions, suggestions and comments. We also thank Isabelle Cantat for supplying the preprints which we cite in this paper and discussing the details of her experiments and simulations. We also acknowledge support from NSF grant IBN-0083653, NASA grant NAG 2-1619, an IBM Innovation Institute award, Indiana University's Pervasive Technologies Laboratory Fellowship and the Biocomplexity Institute.

---

- [1] J.C. Slattery, *A.I.Ch.E. Journal*, 25, 2.283 (1999)
- [2] A.M. Kravnik, *Annu. Rev. Fluid Mech.* 20, 325 (1988).
- [3] D. Weaire and S. Hutzler, *The Physics of Foams*, (Oxford University Press, Oxford, 2000).
- [4] S. Cox, D. Weaire, and J.A. Glazier, *Rheol. Acta* 43, 442 (2004).
- [5] A.D. Gopal and D.J. Durian, *Phys. Rev. Lett.* 75, 2610 (1995).
- [6] D. Weaire and N. Rivier, *Contemp. Phys.* 25, 55 (1984).

[7] H .M .Princen, *J. Colloid Interface Sci.* 91, 160 (1983).

[8] S.A .K han and R .C .A rmstrong, *J. Non-Newtonian Fluid Mech.* 22, 1 (1986); 25, 61 (1987).

[9] D .A .Reinelt and A .M .K raynik, *J. Fluid Mech.* 215, 431 (1990).

[10] K .K awasaki, T .N agai, and K .N akashima, *Philos. Mag. B* 60, 399 (1989); K .N akashima, T .N agai, and K .K awasaki, *J. Stat. Phys.* 57, 759 (1989).

[11] T .O kuzono and K .K awasaki, *Phys. Rev. E* 51, 1246 (1995).

[12] D .J.D urian, *Phys. Rev. Lett.* 75, 4780 (1995); D .J.D urian, *Phys. Rev. E* 55, 1739 (1997).

[13] D .W eaire, F .Bolton, T .H erdtle and H .A ref, *Philos. Mag. Lett.* 66, 293 (1992).

[14] J.A .G lazier, M .P .A nderson and G .S .G rest, *Philos. Mag. B* 62, 615 (1990); J.A .G lazier, *Phys. Rev. Lett.* 70, 2170 (1993); Y .J iang and J.A .G lazier, *Philos. Mag. Lett.* 74, 119 (1996).

[15] Y .J iang, P .J .S wartz, A .S axena, M .A sipauskas and J.A .G lazier, *Phys. Rev. E* 59, 5819 (1999).

[16] C .Z .V an D oom, *J. Appl. Phys.* 46, 3738 (1975).

[17] C .A .H ieber, in *Injection and Compression Molding Fundamentals*, edited by A .I .Isayev, (M aroelD ekker) N ew Y ork, (1987).

[18] O .L ordereau, Ph D thesis, Universite de R ennes, 2002.

[19] I .C antat and R .D elannay, *Phys. Rev. E* 67, 031501 (2003) I .C antat and R .D elannay, *preprint*, (2004).